

See discussions, stats, and author profiles for this publication at: <https://www.researchgate.net/publication/363452339>

# Free from damage beam-to-column joints: Testing and design of DST connections with friction pads

Preprint · April 2021

DOI: 10.31224/osf.io/6rfnz

CITATIONS

0

READS

58

3 authors:



[Massimo Latour](#)

University of Salerno

229 PUBLICATIONS 3,343 CITATIONS

[SEE PROFILE](#)



[Vincenzo Piluso](#)

University of Salerno

287 PUBLICATIONS 7,074 CITATIONS

[SEE PROFILE](#)



[Gianvittorio Rizzano](#)

University of Salerno

253 PUBLICATIONS 4,846 CITATIONS

[SEE PROFILE](#)

# FREE FROM DAMAGE BEAM-TO-COLUMN JOINTS: TESTING AND DESIGN OF DST CONNECTIONS WITH FRICTION PADS

Massimo Latour\*, Vincenzo Piluso & Gianvittorio Rizzano  
University of Salerno  
Civil Engineering Department  
Salerno, Italy  
[mlatour@unisa.it](mailto:mlatour@unisa.it), [v.piluso@unisa.it](mailto:v.piluso@unisa.it), [g.rizzano@unisa.it](mailto:g.rizzano@unisa.it)

## ABSTRACT

Dealing with the seismic behavior of steel MRFs, in last decade, the adoption of dissipative partial-strength beam-to-column joints has started to be considered an effective alternative to the traditional design approach which, aiming to dissipate the seismic input energy at beam ends, suggests the use of full-strength joints. On the base of past experimental results, the use of dissipative Double Split Tee (DST) connections can be considered a promising solution from the technological standpoint, because they can be easily replaced after the occurrence of a seismic event. Nevertheless, their dissipation supply under cyclic loads has been demonstrated to be characterized by significant pinching and strength degradation which undermine the energy dissipation capacity. The need to overcome these drawbacks to gain competitive technological solutions has suggested an innovative approach based on the integration of beam-to-column joints by means of friction dampers located at the beam flange level. Therefore, the use of partial strength DST joints equipped with friction pads is proposed. Aiming to the assessment of the cyclic rotational response of such innovative connections, two experimental programs have been undertaken. The first one has been aimed at characterizing the dissipative performances of five frictional interfaces to be employed as dampers. The second one is aimed at the application of the same materials to DST joints specifically designed for dissipating the seismic input energy in a couple of friction dampers located at the beam flanges level. The results of the experimental analysis carried out at the Materials and Structures Laboratory of Salerno University are herein presented, showing the potential of the proposed damage-free beam-to-column joints.

*Keywords: Friction, Experimental, Design, Joints, Cyclic, Dissipative, Damper, No damage*

*\* Corresponding author*

## 1. INTRODUCTION

According to performance based design, structures in seismic zones have to be designed in order to withstand frequent earthquakes without significant damages and to remain safe, even though a certain amount of structural damage is accepted, in case of seismic events with high return period. In particular, dealing with Moment Resisting steel Frames, according to the most recent seismic codes they can be designed in order to concentrate the energy dissipation capacity at the beam ends (CEN, 2005a) or in the connections (Latour & Rizzano, 2013a; Astaneh-Asl & Nader, 1994; Aribert & Grecea, 2000), even if such second possibility is sometime limited only to the case of ordinary moment frames (AISC, 2010). In the former case, the characteristics of the frame at the Ultimate Limit State (ULS) depend on the plastic rotation capacity and energy dissipation supply of steel members that have to develop wide and stable hysteresis loops (Kato, 1989; Engelhardt et al., 1997; Carter & Iwankiw, 1998; D'Aniello et al. 2012). In the latter case, the energy dissipation supply of the frame depends on the ability of connections to withstand excursions in plastic range without losing their capacity to withstand vertical loads (Awkar & Lui, 1999; Grecea et al., 2004). In such a case, as far as the dissipative capacity of the frame depends on the connections, it is necessary to properly characterize and predict their response under monotonic and cyclic loading conditions (Jaspart, 1991; Bernuzzi et al., 1996; Ermopoulos & Stamatopoulos, 1996; Faella et al., 1998; Faella et al., 2000; Kim & Engelhardt, 2002; Castro et al., 2005; Nogueiro et al. , 2009; Latour et al., 2011; Latour & Rizzano, 2013b).

To this aim, in the last two decades, a number of experimental programs dealing with the characterization of the cyclic behavior of beam-to-column connections have been carried out (Chen et al. 1996; Uang & Bondad, 1996; Whittaker et al., 1996; Yu et al., 2000; Chi & Uang, 2002; Clemente et al., 2004; Ricles et al., 2004; Lignos & Krawinkler, 2007; Dubina et al., 2008; Piluso & Rizzano, 2008; Ramirez et al., 2012). In a work by the same authors, the behavior of four bolted joints, designed to possess the same strength, but detailed to involve in the plastic range different components, has been assessed pointing out the main features of the hysteretic behavior of classical connections (Iannone et al., 2011). Within this activity, Double Split Tee connections have been recognized as an interesting solution to be applied in dissipative semi-continuous MRFs. In fact, DST connections can be easily repaired after destructive seismic events and allow to govern the design process by simply calibrating three geometrical parameters: the width and the thickness of the T-stub flange plate and the distance between the bolts and the plastic hinge arising at the stem-to-flange connection. On

the other hand, beam-to-column joints engaging in plastic range bolted components suffer from several disadvantages. In fact, even though experimental studies demonstrate that bolted components are able to dissipate significant amounts of energy, they have an hysteretic behavior affected by pinching phenomena due to contact phenomena and plastic deformation of the bolts, which usually lead to the deterioration of strength and stiffness of the tee elements.

A possible strategy to overcome the above drawbacks of DST joints has recently been suggested by (Latour & Rizzano, 2012). In particular, in order to improve the hysteretic behavior of DST joints, the authors have proposed to include within the traditional structural detail of DST connections an hysteretic damper realized by cutting the flange plates of the T-stub elements, in the region between the stem and the bolts, according to an hourglass shape similar to the classical ADAS device (Added Stiffness and Damping). In this way, a significant improvement of the performances of DST joints under cyclic loads can be obtained by enhancing the low cycle fatigue resistance of the dissipative joint components. A similar approach, based on the use of hysteretic dampers, has been suggested by (Kim et al., 2007) with reference to joints realized with top and seat angles. In particular, the authors propose to substitute the classical rectangular angle with an hysteretic damper constituted by an angle and a vertical rib in which slits and holes are made in order to concentrate the dissipation in zones specifically designed for absorbing energy.

The use of beam-to-column connections equipped with passive energy dissipation devices has been suggested also by other researchers. In particular, Suita et al. (2004) and Inoue et al. (2006) have proposed the use of Buckling Restrained Braces (BRB) to be connected between the beam flange and the column flange close to the member ends. The top beam flange is pin connected to the column flange, so that the bending moment is transmitted by means of the BRBs axial force acting with a given lever arm. Both double-side bracing configuration and single-side bracing configuration have been proposed for such weld-free beam-to-column connections.

Similarly, Kishiki et al. (2006) have proposed a beam-to-column connection where the top beam flange is connected to the column flange by means of a bolted T-stub, with stiffened stem, fixing the point of rotation while the bottom beam flange is connected to the column flange with a bolted T-stub whose stem has a dog-bone shape and is restrained by an additional plate to prevent its buckling in compression. Therefore, the bottom T-stub is conceived to work as a BRB.

Oh et al. (2009) have proposed the use of a beam-to-column connection typology where the top beam flange is connected to the column flange by means of a fixed bolted T-stub, namely split T, while the bottom beam flange is connected to the column flange by means of a slit damper. The connection is design to behave as a partial strength connection where the energy dissipation capacity is provided by the slit damper.

The use of hysteretic dampers has been also suggested to improve the cyclic response of beam-to-column moment connections for column weak axis. In particular, the connection typology conceived by Koetaka et al. (2005) is characterized by the use of splice plates to connect the top beam flange to a continuity plate welded to the column web and flanges while the bottom beam flange is connected to the continuity plate by means of two omega shaped hysteretic dampers.

More recently, Yeung et al. (2013) have proposed beam-to-column connections with asymmetric friction dampers as connecting elements between the beam bottom flange and the column flange while the center of rotation is fixed by means of a flange plate bolted to the beam top flange and welded to the column flange.

Within the above framework, in this paper a new approach for increasing the energy dissipation capacity of beam-to-column joints of Moment Resisting steel Frames (MRFs) is presented. In particular, it is proposed to modify the classical DST joint detail by adding a friction pad between the T-stub stem and the beam flange which has to be designed in order to prevent its slippage under serviceability limit states and to be activated under severe seismic loading conditions. With the proposed approach the friction mechanism is used to dissipate the seismic input energy and the component method is applied in order to prevent the plastic engagement of other joint components. In addition, because of energy dissipation by friction, the primary connection components practically result free from damage. Therefore, when connections are practically not affected by any damage, non-yielding structures can be designed provided that design criteria rigorously assuring that columns remain in elastic range are applied. Even though the goal of non-yielding structures can be considered a significant advance with respect to traditional moment-resisting frames, it is important to underline that it does not mean that the building is free from damage. In fact, on one hand, it has to be considered that the connections proposed will not snap back to the original configuration, resulting in a permanent drift requiring a recentering in the aftermath of earthquake. On the other hand, large damage could potentially result to non-structural components due to transient and permanent drift. Therefore the connection details between

the structural and non-structural components need to be conceived to accommodate such displacements.

The paper is organized in two parts providing the main results of two experimental activities dealing with the friction components and with the whole beam-to-column joints, respectively. In the first part, with the aim of understanding the potentialities of a number of interfaces to be applied as energy dampers, an experimental study on friction materials is carried out. In particular, three different interfaces are considered: two adopting friction rubber-based materials and one using brass plates, all sliding on steel. All the specimens are clamped by means of high strength bolts and are tested under cyclic loading conditions in order to obtain slippage loads compatible with applications to partial strength joints. In the second part of the work, the same friction materials are applied to an innovative partial strength beam-to-column joint where friction pads are located at the beam flange level. The cyclic behavior of the proposed joints is investigated by means of experimental tests under displacement control on real scale external beam-to-column joints. In particular, as shown in the following, four innovative Double Split Tee (DST) joints are designed aiming to dissipate the seismic input energy by means of the slippage of the stems of the tees on a layer of friction material (Latour et al., 2014), which is interposed between the tee stems and the beam flanges. In this way, under cyclic loading conditions, structural elements do not undergo any damage and the energy dissipation is provided by the alternate movement of the tee stems on the friction pads, which are preloaded by means of high strength bolts.

## **2. EXPERIMENTAL TESTS ON FRICTION MATERIALS**

Preliminarily, in order to investigate the possibility of applying a friction damper within the components of a beam-to-column joint, the frictional properties of different interfaces have been analyzed by designing a sub-assembly to be tested under uniaxial loading conditions. In particular, the tested device is constituted by a layer of friction material that has been placed between plates made of S275 steel (Figure 1). In order to allow the relative movement of the steel on the interposed friction material, one of the inner plates has been realized with slotted holes.

Conversely, the other inner and the two outer plates have been realized with circular holes. The clamping force has been applied by means of 16 M20 bolts 10.9 class (CEN, 2005b) and the holes have been drilled with a 21 mm drill bit. Aiming to evaluate the magnitude of the friction coefficient and the cyclic response, several different layouts of the sub-assembly have been considered varying three parameters: the interface, the tightening torque and the

number of tightened bolts. In particular, the friction characteristics of the following four interfaces have been investigated (Figure 2):

- Steel on steel;
- Brass on steel;
- Friction material M1 on steel;
- Friction material M2 on steel.

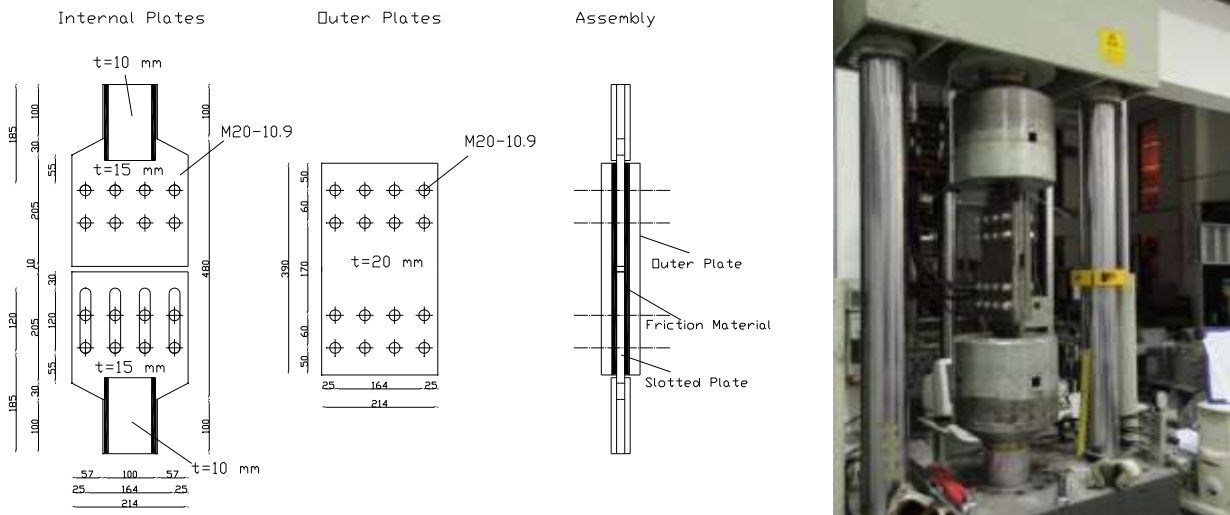


Figure 1: Scheme of the adopted sub-assembly



Steel S275JR



Brass



Material SA-21 (M1)



Material STR-396 (M2)

Figure 2: Surface of the Tested Materials

In addition, in order to evaluate the magnitude of the forces obtained from the experimental tests, the analysis has been carried out by varying the bolt tightening level in the 200 Nm to 550 Nm range, obtaining different values of the clamping force acting on the sliding surface. The main goal of the experimental program is to obtain the friction coefficients of the investigated materials, both static and kinetic, for values of the normal force varying in a range leading to sliding forces suitable for structural applications.

The tests have been carried out by means of a universal testing machine Schenck Hydropuls S56 (Figure 1). The testing equipment is constituted by a hydraulic piston with loading capacity equal to +/- 630 kN, maximum stroke equal to +/- 125 mm and a self-balanced steel frame used to counteract the axial loadings. In order to measure the axial displacements the testing device is equipped with an LVDT, while the tension/compression loads are measured by means of a load cell. The cyclic tests have been carried out under displacement control for different amplitudes at a frequency equal to 0.25 Hz.

The main goals of the experimental campaign are, on one hand, the evaluation of the friction coefficient for different values of the normal force acting on the sliding interface and, on the other hand, the assessment of the cyclic response in order to evaluate the stability of the obtained cycles and the energy dissipation capacity. In the following the test results are discussed reporting the obtained values of the friction coefficient for all the considered interfaces. In particular, starting from the test results, the friction coefficient has been determined as:

$$\mu = \frac{F}{m n N_b} \quad (1)$$

where  $m$  is the number of surfaces in contact,  $n$  is the number of bolts,  $N_b$  is the bolt preloading force and  $F$  is the sliding force. In particular, the bolt preloading force  $N_b$  is determined starting from the knowledge of the tightening torque by means of the following expression:

$$N_b = \frac{T_b}{0.2 d} \quad (2)$$

where  $T_b$  is the value of the tightening torque and  $d$  is the bolt nominal diameter. In next sections the results obtained from the tests of each interface are briefly discussed.

Equation (2) was suggested by the Italian recommendations CNR-UNI 10011 (1997) for the design of steel structures. In addition, according to the data provided by a bolt manufacturer (Fontana, 2004), the application of a tightening torque according to Eq. (2) allows to obtain the prescribed bolt preloading force  $N_b$  with an accuracy of +20%. As a consequence, the



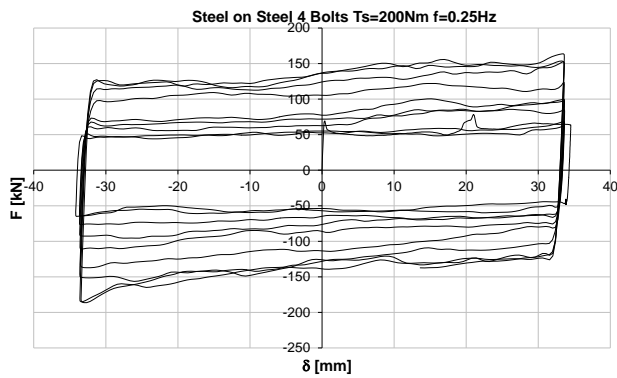
same accuracy is expected regarding the slip resistance of the friction damper. Such scatter is due, on one hand, to the difficulties arising in the control of the tightening torque and, on the other hand, to the variable stiffness of the clamped surfaces. The development of the design rules devoted to beam-to-column joints equipped with friction dampers will need to account for the above uncertainties in the control of the preloading force by establishing appropriate partial safety factors.

## **2.1 *Metallic materials***

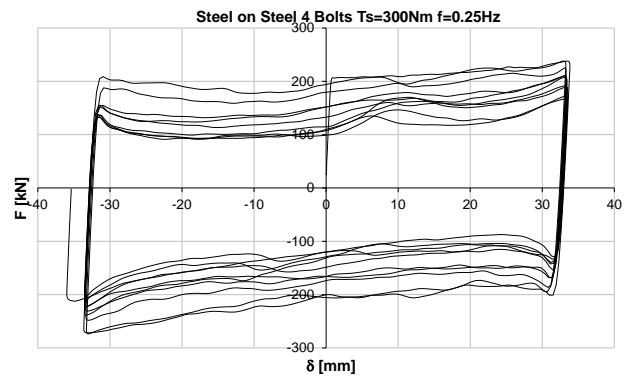
Within the first series of tests two metallic interfaces have been tested, a brass-steel and a steel-steel interface. The specimens have been realized starting from plates made of S275JR structural steel (CEN, 2005a) and CuZn39Pb3 brass alloy. The specimens have been preloaded in each test with different tightening torque levels in order to obtain forces in a range compatible with structural applications. In case of steel-steel interface the tests have been carried out by tightening 4 bolts, in different steps at torques of 200 Nm, 300 Nm and 500 Nm. Conversely, in case of brass-steel interface, the clamping load has been applied by tightening 8 bolts at two different torques: 200 Nm and 300 Nm. Different loading sequences have been applied to the two specimens. In particular, the steel-steel interface has been subjected to 10 loading cycles at the constant amplitude of 30 mm for each one of the desired bolt torques, while the brass-steel interface has been subjected to a sequence of 30 cycles with amplitude of 15 mm for a bolt torque equal to 200 Nm and to a sequence of 20 cycles for a bolt torque equal to 300 Nm. The tightening torques have been applied at the end of each loading sequence by means of a calibrated torque wrench. The main results of the tests are reported in Figure 3.

The results obtained point out that the cyclic behavior of the steel-steel interface is quite unstable. In particular, in the first test (1<sup>th</sup>-10<sup>th</sup> cycle) the specimen exhibited a very steep initial stiffness and after reaching the static sliding force began to slide with a lower force, evidencing that the static coefficient of friction is slightly greater than the dynamic one. However, after few cycles, all the subsequent cycles reached values of the maximum force greater than the initial one. This behavior can be essentially attributed to mechanical interlocking. In fact, initially the surfaces in contact are smooth but, after few cycles of sliding motion, due to the wearing of the steel and to the high contact pressure, the number of asperities increases and the surfaces become rougher. Therefore, the increase of the number of asperities increases the entity of the interlocking friction component. In the second and third loading step, i.e. from 11<sup>th</sup> to 30<sup>th</sup> cycle, the response of the interface is completely

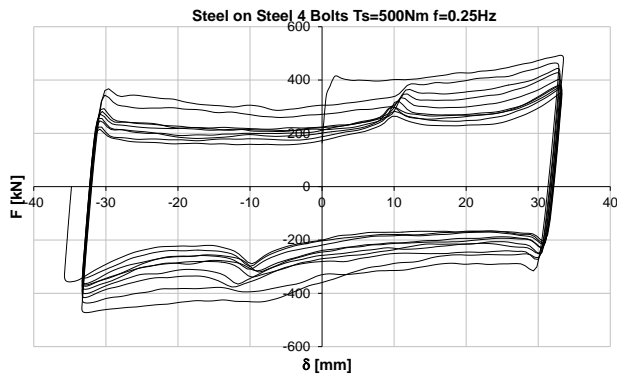
different. In this case, static and dynamic sliding loads assume similar values and the maximum slippage force experienced during the whole loading history is reached during the first cycle. In fact, it is possible to observe a continuously softening behavior which is due to the wearing of the steel and, as a consequence, to the loss of the bolt preload. In case of brass-steel interface the behavior is characterized by a first sliding force quite lower compared to steel-steel interface but, nevertheless, as the number of cycles increases the sliding force also increases exhibiting an hardening behavior.



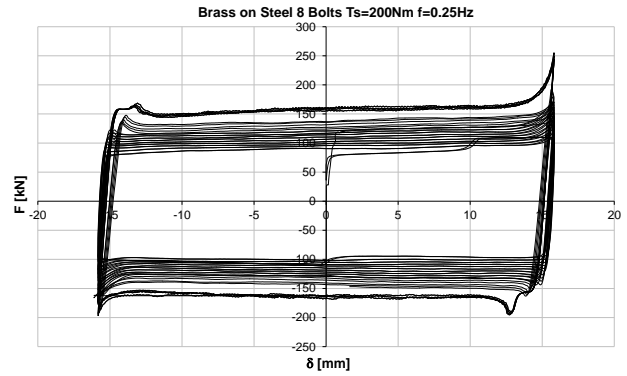
Steel-Steel - Cycles 1-10 ( $T_s=200\text{Nm}$ )



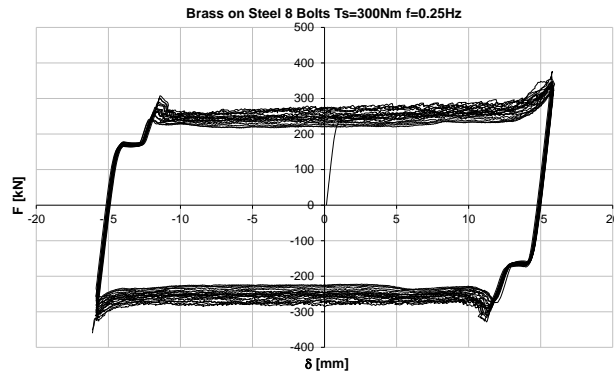
Steel-Steel - Cycles 11-20 ( $T_s=300\text{Nm}$ )



Steel-Steel - Cycles 21-30 ( $T_s=500\text{Nm}$ )



Brass-Steel - Cycles 1-30 ( $T_s=200\text{Nm}$ )



Brass-Steel - Cycles 31-50 ( $T_s=300\text{Nm}$ )

Figure 3: Cyclic response of friction pads with metallic interface

In Figure 4 the experimental results are also represented in terms of non-dimensional force, determined as  $\bar{F} = F / (m n N_b)$ . This non-dimensional force is coincident with the friction coefficient when first sliding occurs. Conversely, in the following cycles, it is the result of complex phenomena involving the variation of asperity interlocking and ploughing conditions and the variation of the bolt preloading force due to the wearing of the contact surfaces. It is possible to observe that the static coefficient of friction of steel-steel interface (0.173) is higher than the brass-steel interface (0.097). Furthermore, with reference to steel-steel interface, in the first loading sequence, after few cycles, the non-dimensional force increases up to a value equal to 0.344 and in the subsequent loading histories starts from a value approximately equal to 0.35-0.40 and then quickly decreases at a value of about 0.20. In case of brass-steel interface during the first loading sequence, i.e. from the 1<sup>st</sup> to the 60<sup>th</sup> cycle, the non-dimensional force starts from a value of 0.097 and at the end of the test increases up to about 0.20. In the second step of the loading sequence, i.e. from the 61<sup>th</sup> to the 100<sup>th</sup> cycle, the non-dimensional force continues to increase up to the value of about 0.23.

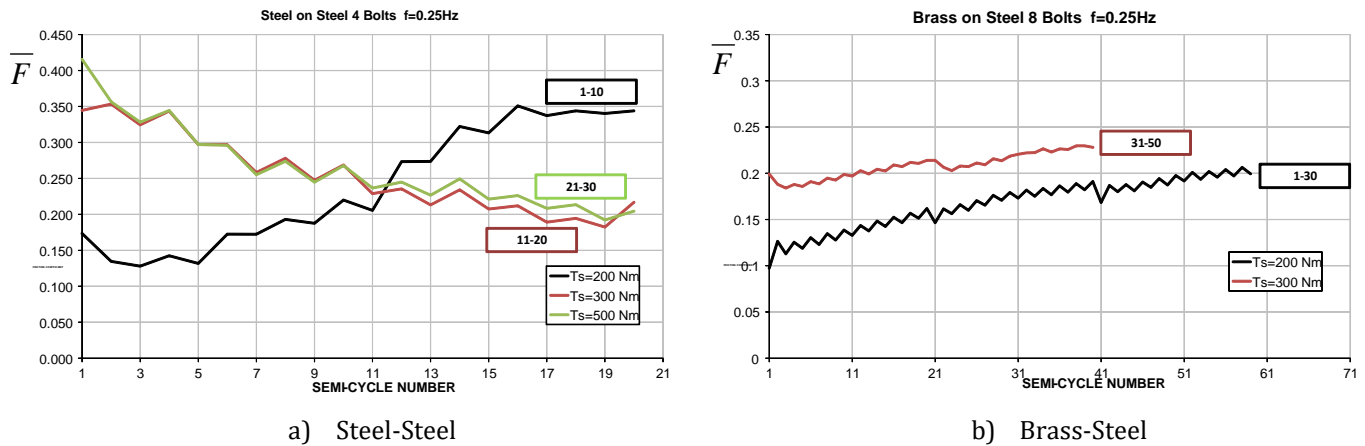


Figure 4: Non-dimensional force versus semi-cycles for metallic interfaces

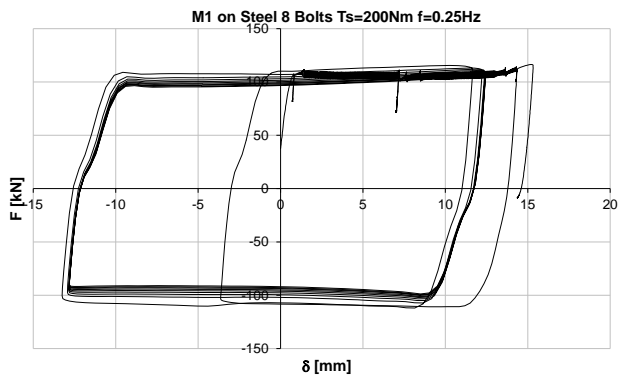
## 2.2 Rubber materials

The rubber materials investigated in this work are both composed by a blend of nitrilic rubbers and phenolic resins where a mix of mineral, steel and synthetic fibers is included. Two materials have been tested, both produced by the Italian factory “Brake Project srl”. The first one is the friction material SA-21 (material M1 in the following), which is normally employed as braking material for electric motors. It is characterized by a density of 2,150 g/cm<sup>3</sup> and superficial hardness equal to 75 Shore D. The second material is named STR-396 (material M2 in the following) and has the particularity to include within its thickness a mesh

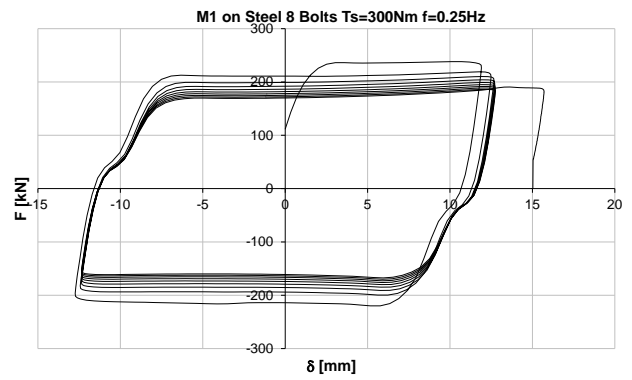
made of copper. It is a material characterized by a high resistance to abrasion, due to the high value of hardness equal to 85 Shore D, and density equal to  $1,8 \text{ g/cm}^3$ .

Dealing with material M1, four tests with 8 bolts tightened at torques of 200, 300, 400 and 550 Nm have been carried out. The adopted loading sequence has provided 10 cycles at amplitude of  $\pm 10 \text{ mm}$  for each loading step of the displacement history. Concerning material M2, three tests with 8 bolts tightened at torques of 200, 300 and 400 Nm and 10 cycles at amplitudes of  $\pm 15 \text{ mm}$  have been carried out. The results of the tests, reported in Figure 5, point out that M1-steel interface provides a quite stable response for low values of the tightening torque but, for values higher than 300 Nm significant stiffness and strength degradation are exhibited. This behavior is due to the low tensile resistance of the friction material which in fact, after the 4<sup>th</sup> loading sequence collapsed with the development of a crack at the transversal section weakened by the hole, leading to the complete fracture of the friction pad. The M2-steel interface provided a very stable response. In the first loading sequence, i.e. cycles from 1<sup>th</sup> to 10<sup>th</sup>, after the first cycle a slight hardening behavior has been exhibited. In the second test, namely cycles from 11<sup>th</sup> to 20<sup>th</sup>, a stable behavior has been provided with almost the same value of the sliding force in all the cycles. Only in the third loading sequence, a softening behavior was exhibited probably due to the high contact pressure.

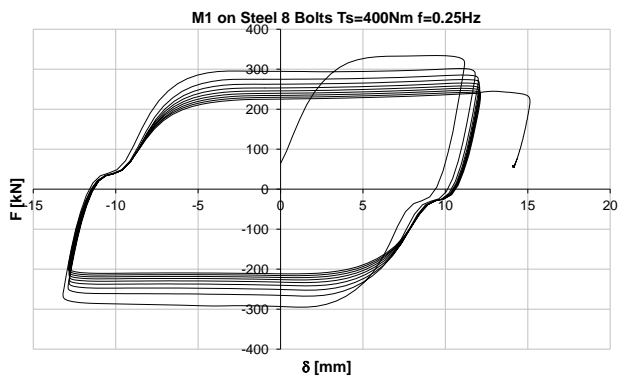
The results obtained are also represented in Figure 6, with the same procedure previously shown, in terms of non-dimensional force. From this figure, it is apparent that the initial values of the non-dimensional force of the investigated rubber materials, vary in the range contained between 0.15 and 0.2. The main difference between the two material is due to the different response as far as the number of cycles increases. In fact, in case of material M1 the response after the first sliding is always softening in the whole range of investigated contact pressure. Conversely, material M2 provides a better response, especially at low values of the tightening torque, because of hardening response or constant sliding force. The above differences are mainly due to the higher hardness of the material and to the copper mesh included in the thickness of the plate which lead to a higher resistance to abrasion and to a higher tensile resistance of the material, respectively.



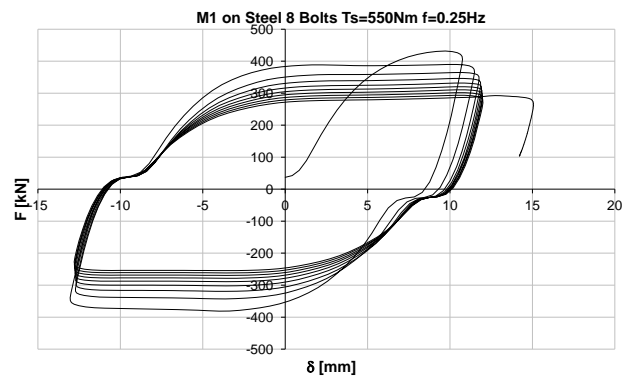
M1-Steel interface- Cycles 1-10 ( $T_s=200\text{Nm}$ )



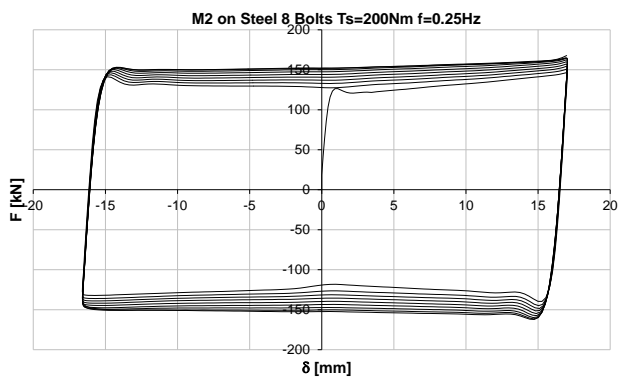
M1-Steel interface - Cycles 11-20 ( $T_s=300\text{Nm}$ )



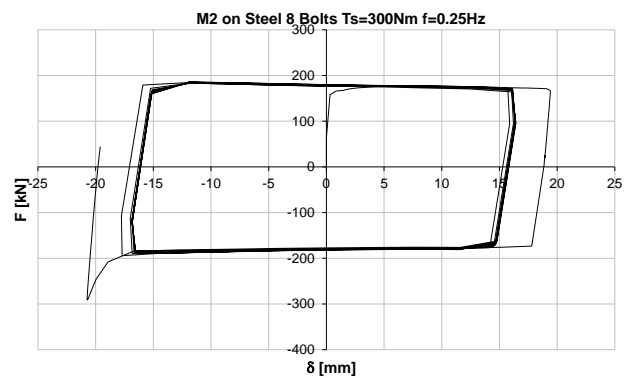
M1-Steel interface - Cycles 21-30 ( $T_s=400\text{ Nm}$ )



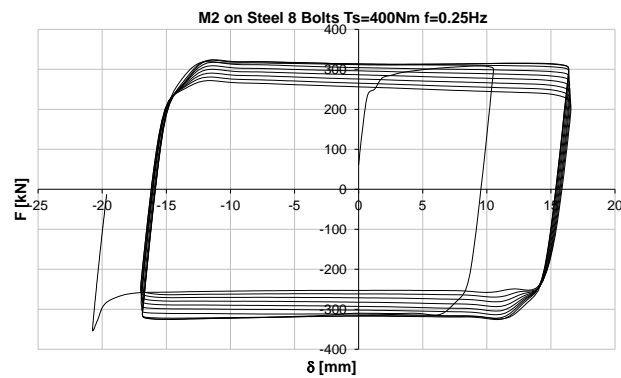
M1-Steel interface - Cycles 31-40 ( $T_s=500\text{ Nm}$ )



M2-Steel interface - Cycles 1-10 ( $T_s=200\text{Nm}$ )



M2-Steel interface - Cycles 11-20 ( $T_s=300\text{Nm}$ )



M2-Steel interface- Cycles 21-30 ( $T_s=400\text{ Nm}$ )

Figure 5: Cyclic response of friction pads with rubber materials

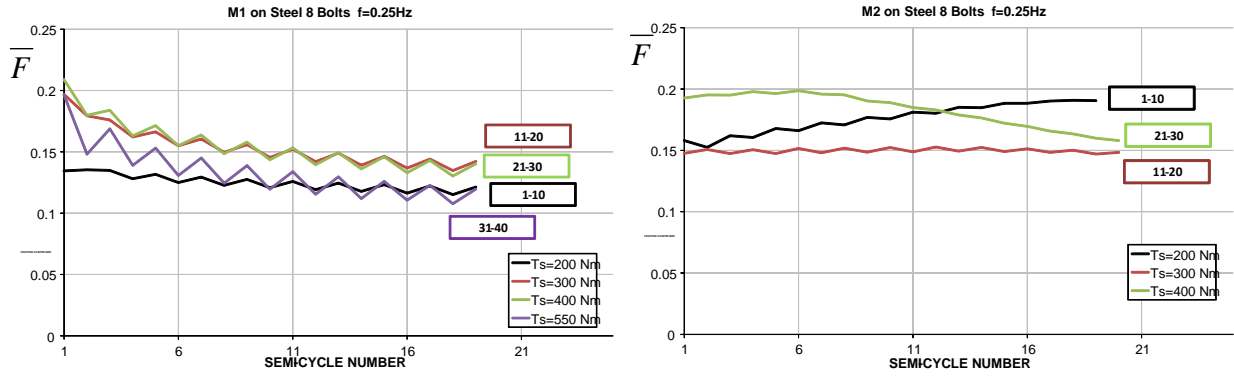


Figure 6: Non-dimensional force versus semi-cycle for rubber-steel interfaces

### 3. CONCEPTION AND DESIGN OF THE TESTED SPECIMENS

Starting from the behavior of the sub-assemblages studied in the previous section, the design of dissipative DST connections with friction pads has been performed. As previously mentioned, in this paper it is proposed to improve the classical detail of Double Split Tee connections by adding friction dampers within the joint detail. In particular, the use of slotted holes on the tee stem and the location of a friction pad between the stem and the beam flange allows to provide the connection with a friction damper (Fig. 7). The slip resistance of the friction damper has to be designed so that the connection is able to withstand a bending moment less than the beam plastic resistance. Therefore, the yielding of the beam end is prevented and also the beam-to-column connection results free from damage, provided that the connection components are designed to exhibit a resistance greater than the slip resistance of the friction damper. Such slip resistance is simply obtained as the ratio between the desired bending resistance and the lever arm. In order to control the slip resistance at the interface, analogously with the sub-assemblage already studied, the interface is pre-stressed by means of high strength bolts whose tightening torque is properly calibrated according to Eq. (1) and Eq. (2) to obtain the desired  $F$  value for a given number of bolts and a given friction coefficient.

In this paper, in order to investigate the potential of the proposed approach, the performance of such innovative DST connections with friction pads under cyclic loading conditions is compared with the hysteretic characteristics of a traditional double split tee connection tested in a previous work (Iannone et al., 2011), namely TS-CYC 04. Such a specimen is a T-stub joint dissipating the energy in a couple of rectangular T-stubs which are designed to be the weakest joint component. Therefore, the beam-column coupling selected in this work is the same used for test TS-CYC 04, consisting in an HEB 200 column fastened to an IPE 270 beam, the first made of S275 steel, the second made of S355 steel.

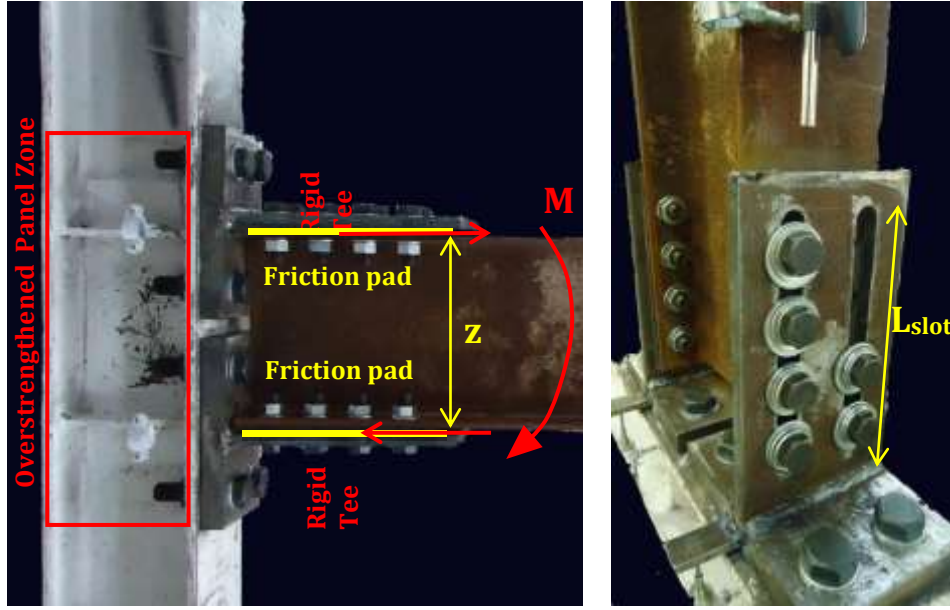


Figure 7: Concept of the tested joint

Within the framework of the component method, with reference to the proposed innovative DST connections the following components can be identified: the panel zone in shear, the column web panel zone in tension and compression, the T-stubs and the friction dampers. In order to reach the design goal, the joint components of the DST connection have to be designed with sufficient overstrength with respect to the maximum force that the friction dampers are able to transmit. According to this hierarchy criterion, starting from the knowledge of the design bending moment, the geometry of all the elements composing the connection can be defined by exploiting formulations provided by literature models or by the formulations contained in Eurocode 3 (CEN 2005b, 2005c).

The design resistance is the same assumed for joint TS-CYC 04, i.e.  $M_{Rd} = 100 \text{ kNm}$  (Iannone et al., 2011) leading to a partial strength ratio with respect to the connected beam equal to 0.75 (IPE 270 -  $M_{pb} = 133 \text{ kNm}$ ). All the joint components, with the only exception of the friction pad, have to be designed with sufficient overstrength to avoid their yielding.

Dealing with the column panel zone in shear, in order to avoid its plastic engagement, a couple of 10 mm doubler plates welded on the column web has been adopted. In particular, the shear panel has been designed by means of Kim and Engelhardt's model (2002) accounting for the additional resistance due to the doubler plates. According to this model, the yield strength of the panel zone  $M_y$  can be evaluated as the product of three terms:

$$M_y = K_e C_y \gamma_y \quad (3)$$

where  $K_e$  is the elastic stiffness,  $C_y$  is the average shear deformation factor accounting for the distribution of shear stresses in the panel zone at yielding and  $\gamma_y$  is the shear deformation.

According to Kim & Engelhardt's model (2002), the elastic stiffness  $K_e$  can be computed considering both the shear stiffness of the column web panel  $k_b$  and the contribution due to the flexural stiffness of the column flanges  $k_s$ , respectively given by:

$$k_b = \frac{C_r EI_c}{[(d_b - t_{bf})/2]^3} = \frac{5 \cdot 210000 \cdot 56960000}{[(270 - 10)/2]^3} = 27222576 \text{ N/mm} \quad (4)$$

$$k_s = \frac{G(A_{vc} + A_{dp})}{[(d_b - t_{bf})/2]} = \frac{80769 \cdot (2483 + 3700)}{[(270 - 10)/2]} = 3841498 \text{ N/mm} \quad (5)$$

where  $C_r$  is a restraint factor accounting for the boundary conditions of the column flanges assumed equal to 5,  $E$  and  $G$  are the elastic and the shear modulus respectively,  $I_c$  is the moment of inertia of the column section,  $d_b$  is the beam depth,  $A_{vc}$  is the column web shear area and  $A_{dp}$  is the shear area of doubler plates, defined as the product of the thickness (10 mm) multiplied for the width of the doubler plates (185 mm). Therefore, the rotational stiffness of the panel zone in shear is given by (Kim and Engelhardt, 2002):

$$K_e = \frac{k_b k_s}{k_b + k_s} \frac{(d_b - t_{bf})}{2} \frac{(d_b - t_{bf})}{\beta} = \frac{27222576 \cdot 3841498}{27222576 + 3841498} \frac{(270 - 10)^2}{2 \cdot 1} = 1.137 \cdot 10^{11} \text{ Nmm} \quad (6)$$

according to Kim and Engelhardt,  $C_y$  varies in the range 0.8-0.9, so that for design purposes, the mean value  $C_y = 0.85$  can be adopted. Regarding  $\gamma_y$ , taking into account that for the tested specimens a constant axial force ( $P$ ) equal to 30% of the squash load ( $P_y$ ) has been applied, according to von Mises yield criterion, the shear deformation at yielding is given by:

$$\gamma_y = \frac{f_y}{\sqrt{3}G} \sqrt{1 - \left(\frac{P}{P_y}\right)^2} = \frac{355}{\sqrt{3} \cdot 80769} \sqrt{1 - (0.3)^2} = 0.00242 \quad (7)$$

As a consequence, the shear panel resistance can be computed as:

$$M_{pz} = 1.137 \cdot 10^{11} \cdot 0.85 \cdot 0.00242 = 233.9 \cdot 10^6 \text{ Nmm} \approx 234 \text{ kNm} \quad (8)$$

Therefore, by adopting the doubler web plates, the shear panel resistance is greater than the joint design resistance of a factor higher than 2, so that it is expected that the panel zone remains in the elastic range up to the slippage of the friction dampers. In order to prevent the yielding of the T-stubs, they are designed to withstand a tensile force equal to the design bending moment divided by the lever arm multiplied for an overstrength coefficient equal to 1.5:

$$F_{T-stub} = \frac{M_d}{z} = 1.5 \frac{100000}{286} = 530 \text{ kN} \quad (9)$$

where  $z$  is evaluated as the distance between the friction pads. Assuming that the T-stub fails according to mechanism type-1 of Eurocode 3, its plastic resistance can be determined as the



sum of the plastic resistances of the two bolt rows which, in the present case, are characterized by different values of the distance  $m$  between the bolt row and the T-stub web:

$$F_{T-stub} = \frac{b_{eff} t_p^2}{m_1} f_y + \frac{b_{eff} t_p^2}{m_2} f_y \quad (10)$$

where, according to the T-stub geometry,  $b_{eff}$  is the effective width assumed as equal to one half of the total T-stub width (85.5 mm),  $m_1$  is equal to 63 mm,  $m_2$  is equal to 78.9 mm,  $t_p$  is the plate thickness and  $f_y$  is the yield strength of the plate equal to 275 MPa. Therefore,  $t_p$  can be determined as:

$$t_p = \sqrt{\frac{F_{T-stub} \left( \frac{m_1 m_2}{m_1 + m_2} \right)}{b_{eff} f_y}} = \sqrt{\frac{530000 \left( \frac{63 \cdot 78.9}{63 + 78.9} \right)}{85.5 \cdot 275}} = 28.1 \text{ mm} \quad (11)$$

As a consequence, a 30 mm thick plate has been selected for the T-stub flange. The bolts fastening the T-stub flange to the column have been designed in order to guarantee type-1 collapse mechanism. In particular, according to the component method it is well known that this condition is satisfied if the following inequalities are verified:

$$\frac{b_{eff} t_p^2 f_y}{2B_{Rd} m_1} \leq \frac{2n/m_1}{1 + 2n/m_1} \quad \frac{b_{eff} t_p^2 f_y}{2B_{Rd} m_2} \leq \frac{2n/m_2}{1 + 2n/m_2} \quad (12)$$

where  $n$  is the distance between the bolts axis and the free edge of the T-stub flange, assumed equal to 45 mm. By means of Eq. (12), the design of the bolts has been carried out as follows:

$$B_{Rd} \geq \frac{(1 + n/m_1) b_{eff} t_p^2 f_y}{4n} = 201.5 \text{ kN} \quad B_{Rd} \geq \frac{(1 + n/m_2) b_{eff} t_p^2 f_y}{4n} = 184.6 \text{ kN} \quad (13)$$

M27 bolts made of 10.9 class have been adopted. Concerning the panel zone in tension and compression a couple of continuity plates with a thickness equal to the beam flange thickness has been adopted, thus assuring that the column web in tension and the column web in compression remain in elastic range.

Dealing with friction dampers, they have to be designed in order to allow the slippage of the friction pad on the T-stub web. To this scope, the length of the slotted holes has to be properly designed as a function of the desired value of the joint rotation capacity. This can be easily determined by the following equation:

$$L_{slot} = (n_{br} - 1)p + d_b + 2\phi z \quad (14)$$

where  $d_b$  is the bolt diameter,  $n_{br}$  is the number of bolt rows used to fasten the web of the T-stub to the beam flange,  $p$  is the bolt pitch and  $\phi$  is the design value of the joint rotation

capacity. By adopting eight M20 bolts located according to four rows, with a spacing equal to 60 mm and by assuming a design joint rotation equal to  $\pm 70$  mrad, it follows:

$$L_{slot} = (4 - 1)60 + 20 + 2 \cdot 0.07 \cdot 286 = 240 \text{ mm} \quad (15)$$

The bolt preloading level has been assumed equal to 460 Nm.

The geometry of the specimen resulting from the above design criteria is depicted in Fig. 8.

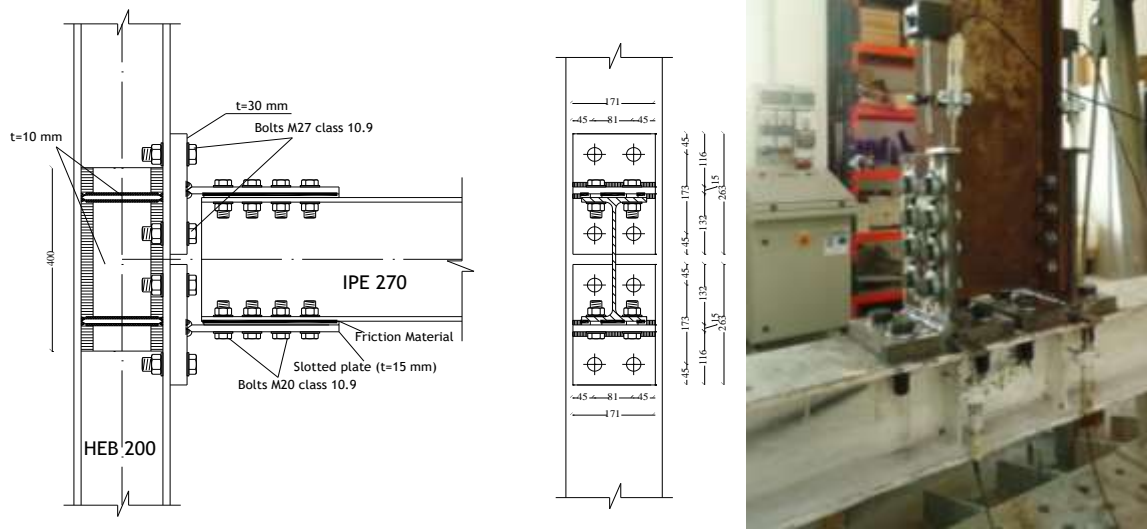


Figure 8: Geometry of the tested specimens

#### 4. EXPERIMENTAL LAYOUT

Experimental tests on the proposed device have been carried out at Materials and Structures Laboratory of Salerno University. Two steel hinges, designed to resist shear actions up to 2000 kN and bolted to the carriage base have been employed to connect the specimens to the reacting system. The specimens are assembled with the column (HEB 200) in horizontal position, connected to the hinges, and the beam (IPE 270) in vertical position (Figure 9). The loads have been applied by means of two different hydraulic actuators. The first one is a MTS 243.60 actuator with a load capacity equal to 1000 kN in compression and 650 kN in tension with a piston stroke equal to  $\pm 125$  mm which has been used to apply, under force control, the axial load in the column equal to the 30% of the squash load. The second actuator is a MTS 243.35 with load capacity equal to 250 kN both in tension and in compression and a piston stroke equal to  $\pm 500$  mm which has been used to apply, under displacement control, the desired displacement history at the beam end. In order to avoid the lateral-torsional buckling of the beam an horizontal frame has been employed. The geometry of the frame is defined in order to work as a guide which restrains the lateral displacement of the beam and allows the beam rotations. The loading history has been defined in terms of drift angle, according to the protocol provided by AISC (2005).

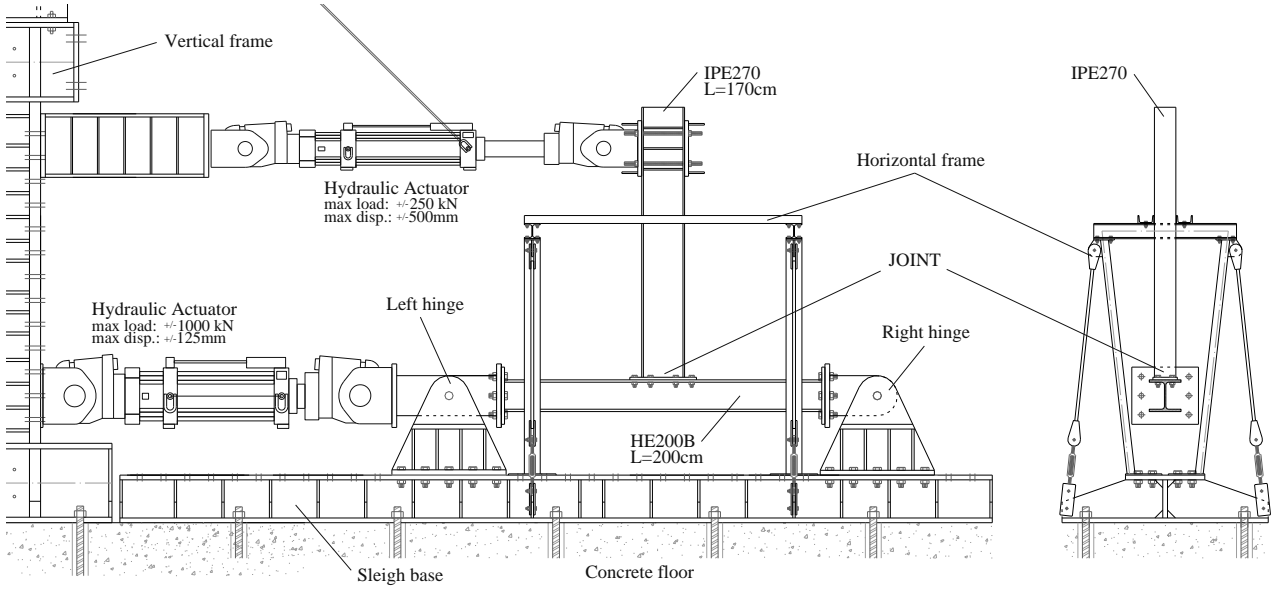


Figure 9: Experimental Setup for tests on joints

During the tests many parameters have been monitored and acquired, in order to get the test machine history imposed by the top actuator and the displacements of the different joint components.

Aiming at the evaluation of the beam end displacements due to the beam-to-column joint rotation only, the displacements measured by means of the LVDT equipping MTS 243.35 have been corrected by subtracting the elastic contribution due to the beam and column flexural deformability according to the following relationship:

$$\delta_j = \delta_{T3} - \frac{FL_b^3}{3EI_b} - \frac{FL_c L_b^2}{12EI_c} \left[ \left( \frac{L_c}{L_c + 2a} \right)^2 + \frac{6a}{L_c + 2a} \right] \quad (16)$$

where  $I_b$  and  $I_c$  are the beam and column inertia moments,  $L_c$  is the column length,  $L_b$  is the beam length and  $a$  is the length of the rigid parts, due to the steel hinges (Figure 10).

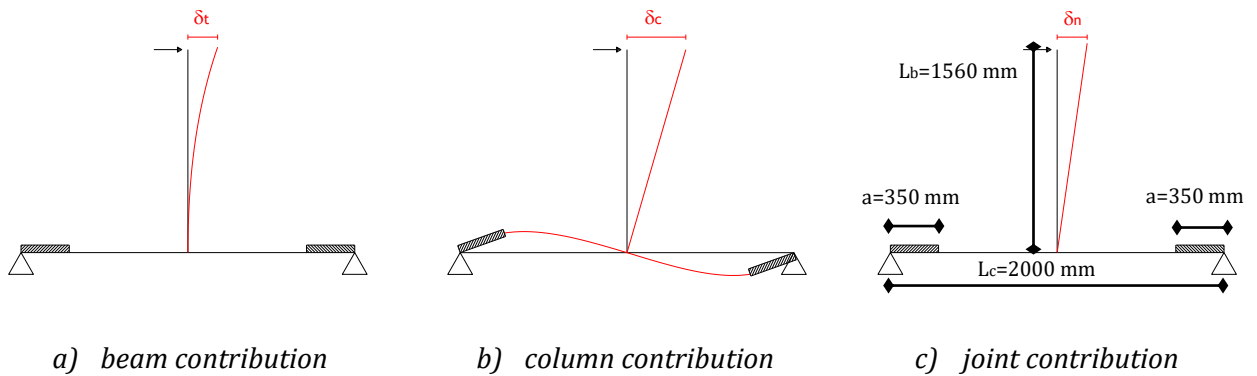


Figure 10: Scheme for evaluating the joint contribution to the overall rotation

The experimental program carried out concerns four specimens, namely TSJ-M1-CYC08, TSJ-M2-CYC09, TSJ-M2-DS-CYC10 and TSJ-B-CYC11, which are four double split tee connections. The first three with layers of friction material, namely M1 and M2, and the fourth one with a brass plate interposed between the Tee stems and the beam flanges. The slipping interfaces have been clamped by means of eight M20 class 10.9 bolts tightened with a torque equal to 460 Nm. In order to allow the relative movement between the stems of the T-stubs and beam flanges, two slotted holes have been realized on the tee stems. As previously said, the slots have been designed in order to allow a maximum rotation of 70 mrad. The flanges of the T-stubs are fastened to the column flanges by means of eight M27 class 10.9 bolts put into holes drilled with a 30 mm drill bit. As better explained in next section, joint TSJ-M2-DS-10 has the particularity to employ annular disc springs which are interposed between the bolt nut and the beam flange;

The identification label of the tests refers to the following issues: 1- Joint typology, i.e. Tee Stub Joint (TSJ) / 2 – Friction interface, i.e. Friction material M1 (M1), Friction material M2 and Brass (B) / 3 – Type of washer employed in the test (DS stands for Disc Spring) / 4 – Progressive number of cyclic tests, i.e. CYCXX.

## **5. CYCLIC BEHAVIOR OF SPECIMENS**

As aforementioned, the main goal of the work here presented is to provide an innovative approach to the seismic design of beam-to-column joints. In particular, it is well known that dissipative zones in seismic resistant moment frames are typically located at the beam ends where the dissipation of the earthquake input energy is expected. Such dissipation traditionally occurs at the ends of the structural member where the development of plastic hinges are expected, provided that full-strength beam-to-column joints are adopted. As a consequence, structural damage results from such dissipation. The alternative approach, consisting in the use of semirigid partial-strength beam-to-column joints, prevents the damage of the structural members, but the main source of energy dissipation is provided by the plate connecting elements of the bolted components so that damage occurs in the connection components. Aiming to the development of free from damage connections, the beam-to-column joint typology herein proposed is detailed in order to dissipate the seismic input energy through the slippage of the material, i.e. the friction pad, interposed between the T-stub stem and the beam flange. From the design point of view, this aim is obtained by applying hierarchical criteria at the level of the joint components. In particular, the T-stubs,

the bolts and the column panel zone have been designed with sufficient overstrength with respect to the dissipative component, i.e. the friction pad, which has been designed to slip at a force level corresponding to the design bending moment equal to 100 kNm. The desired force at the sliding interface has been reached by properly tightening the bolts fastening the tee stems to the beam flanges.



Figure 11: Relative displacement between the beam flange and the T-stub web observed during the tests

As expected on the basis of the design criteria adopted, in all the experimental tests there has not been any damage of the joint components, but only the wearing of the friction pads. Therefore, a very important result coming from the experimental program is the confirmation that this connection typology can be subjected to repeated cyclic rotation histories, i.e. to repeated earthquakes, by only substituting the friction pads, if needed, and by tightening again the bolts to reach the desired preloading level. In addition, the rotation capacity can be easily calibrated by simply governing the length of the slotted holes. In fact, in all the tests the rotation demand applied to the joint has been completely due to the slippage of the friction material on the T-stub web (Figure 11).

The experimental results are in line with the results pointed out in the tests on the friction interfaces pointing out that, as expected, the cyclic behaviour of the joint is mainly governed by the cyclic behaviour of the friction damper.

In test TSJ-M1-CYC08, where material SA-21 was employed, the response of the joint has been very similar to that exhibited during the uniaxial tests on the interface (Figure 12). In particular, at low force values the joint exhibited an elastic behaviour. When a bending moment level approximately equal to the design one is reached, the slippage of the friction dampers starts. However, the cyclic behaviour of this joint has been quite poor, mainly due to

the low tensile strength of the friction material which failed at a value of the rotation amplitude relatively low, equal to about 20 mrad. In particular, the joint failure occurred due to the collapse of the rubber plate in the zone weakened by the holes (Figure 13). The hysteretic behaviour of joint TSJ-M1-CYC08, after the slippage of the friction dampers, has been affected by significant pinching and strength degradation phenomena due to the reduction of the bolt preloading force after the fracture of the rubber plate. From the results obtained it is possible to conclude that this rubber material is not suitable for the application to friction dampers to be used in double split tee joints where high values of the contact pressure are needed (Fig. 14).



Figure 12: Test TSJ-M1-CYC 08

Conversely, the joint equipped with friction pads made of material STR-396 (M2) exhibited a better response. In particular, also in this case, the hysteretic behavior of the joint has been mainly governed by the response of the friction dampers obtaining, as already observed in tests on the joint component, wide and stable hysteretic loops. For bending moment levels less than the design resistance, the cyclic behaviour has been characterized by loading and unloading elastic branches.



Figure 13: Failure of the rubber plate in test TSJ-M1-CYC08

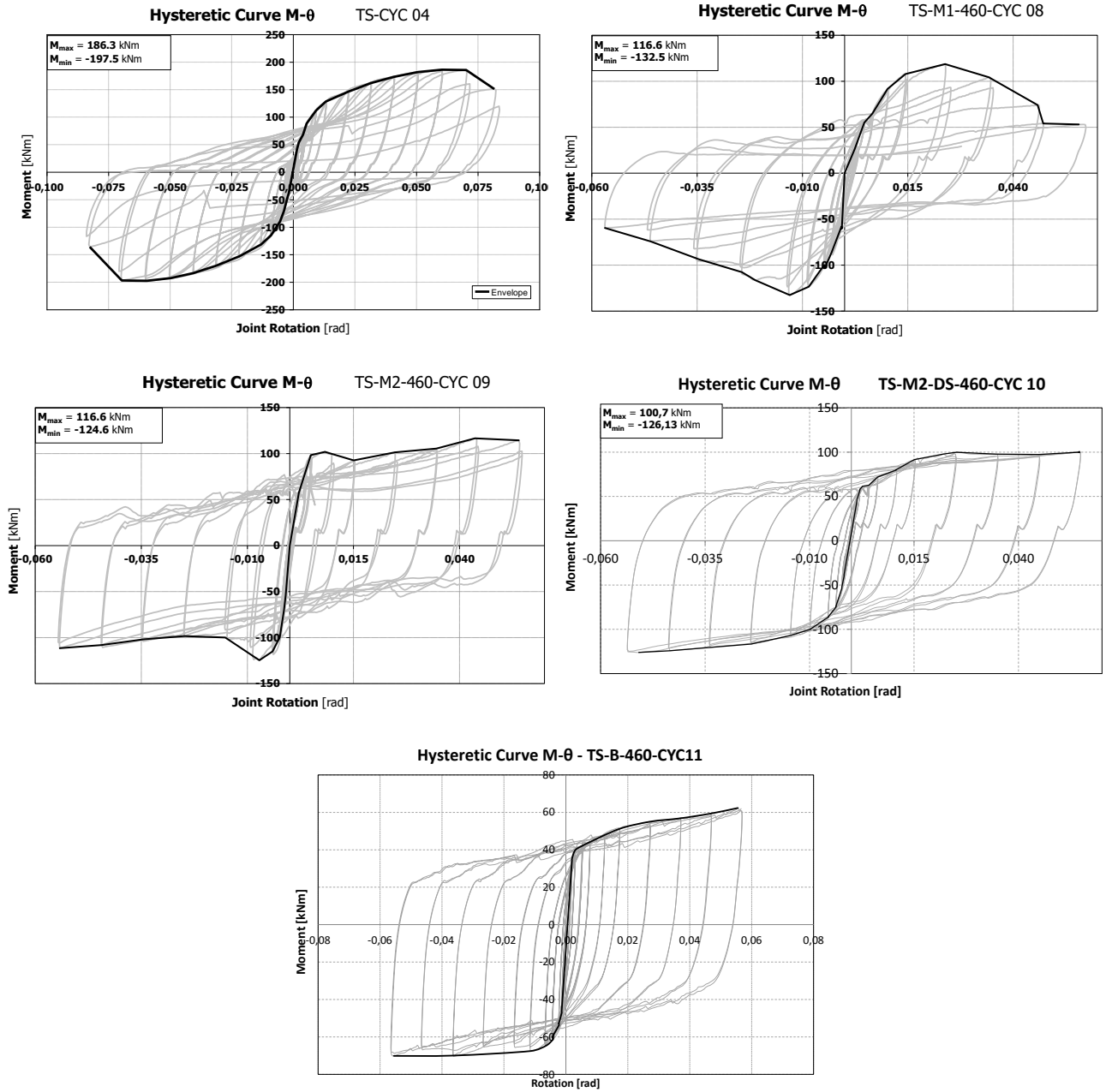


Figure 14: Hysteretic curves of tested joints

After the attainment of a bending moment value approximately equal to 100 kNm, the slippage of the friction dampers occurs (Fig. 14). In this phase, the joint hysteretic response has been characterized by cycles with a parallelogram shape (Fig. 14). It is useful to note, from the comparison with the response of tests on friction dampers, that the shape of the hysteresis cycle of the friction DST joint differs from that observed during the uni-axial tension test. This difference is mainly due to the role played by the beam rotation in the kinematic mechanism. In fact, the beam rotation causes two effects that give rise to an



increase of the bending moment as far as the beam rotation increases. On one hand, there is an increase of the local pressure on the friction pads due to the reaction force provided by the T-stub webs that behave in a way similar to a pocket foundation. On the other hand, minor yielding of the tee stems at the web-to-flange attachment contributes to the total bending resistance of the joint. Both of these effects lead to the hardening behaviour experimentally observed (Fig. 14). Moreover, the results of test TSJ-M2-CYC09 (Fig. 15) show that, at high rotation amplitudes, slight strength and stiffness degradation occurs, probably due to the consumption of the friction pads during the sliding motion.

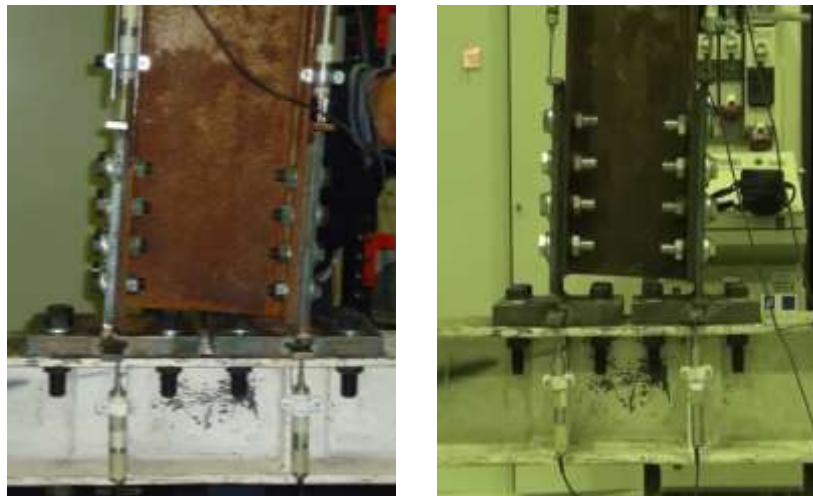


Figure 15 – Tests TSJ-M2-CYC09 (left) and TSJ-M2-DS-CYC10 (right)

Starting from the behaviour previously observed, another test with the same layout but adopting disc springs interposed between the bolt head and the tee web plate has been carried out (TSJ-M2-DS-CYC10) (Fig. 15). In this way, it was expected that the pinching and degradation behaviour due to the wearing of the friction material observed during test TSJ-M2-CYC09 is overcome. This particular type of washer is a high resistance cone shaped annular steel disc spring which has a behaviour very similar to a classical spring. In fact, it flattens when compressed and returns to its original shape if compression loading is released (Heistermann, 2011; Schnorr, 2003). In this way, as the friction material wears, leading to the partial loss of bolt preload, the disc spring restores the force by maintaining the bolt shank in tension. The results of test TSJ-M2-DS-CYC10 demonstrate the effectiveness of the adopted disc springs. In fact, the obtained cyclic behaviour is very similar to that exhibited by specimen TSJ-M2-CYC09, but a higher dissipation capacity and lower strength and stiffness degradation was obtained (Fig. 14).

Test on Brass TSJ-B-CYC11 (Fig. 16) also exhibited a satisfactory behaviour in terms of shape of the cyclic response. In fact, the cycles obtained have been very stable also at high values of



the plastic rotation. Nevertheless, a value of the bending moment less than the design value equal to 100 kNm was obtained. This result can be justified on the base of the results obtained on the subassemblage. In fact, in case of brass on steel interface the value of the static friction coefficient is much lower than the dynamic one and, as a consequence, a bending moment lower than the expected one has been obtained (Fig. 14).



Figure 14: Substitution of the rubber plate with the brass plate

In order to compare the cyclic behavior of DST connections with friction materials to that of a traditional partial-strength joint dissipating in the bolted components and characterized by the same resistance (TS-CYC 04), the envelopes of the cyclic moment-rotation curves are reported in Figure 15. It can be observed that the bending moment values corresponding to the knee of the curves, corresponding to the design value of the joint resistance, are similar, but the post-elastic behaviours are quite different. In fact, compared to the case of joint TS-CYC 04, friction DST joints do not exhibit significant hardening behaviour. With reference to TS-M2-CYC09 and TS-M2-DS-CYC10 tests, it is worth to note that the hysteresis cycles are wide and stable with no pinching. This is the reason why the joints, in spite of the less hardening behavior, are able to dissipate more energy than connection TS-CYC04.

## CONCLUSIONS

Within this paper, the results of two experimental programs devoted to understand the possibility to apply friction materials to supplemental damping devices and to friction pads equipping beam-to-column joints have been presented. In a first part of the work, the response under tension/compression loads of an isolated friction damper has been analyzed.

In particular, two metallic and two rubber materials have been tested. The main results of the first experimental program can be summarized as follows:

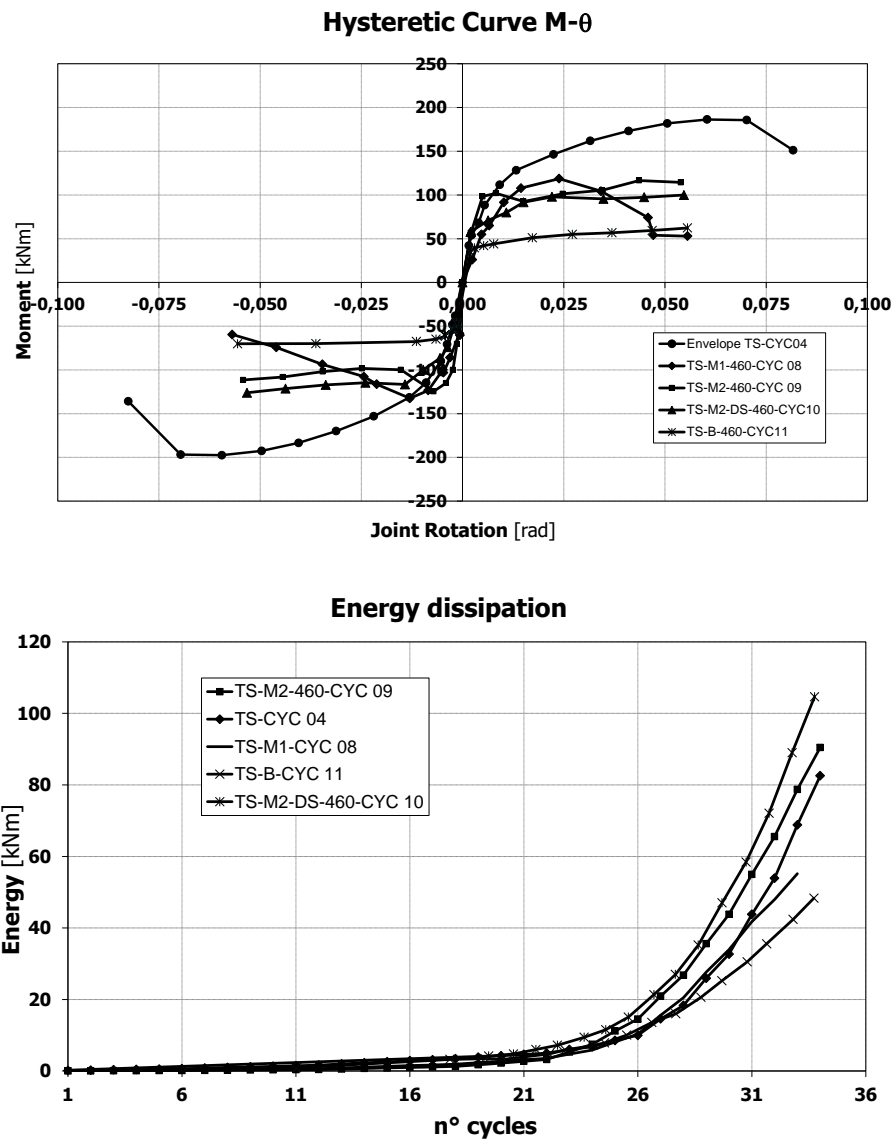


Figure 15. Cyclic Envelopes and Energy Dissipation of Tested Joints

- Steel on steel interface exhibited high coefficient of friction, but a quite unstable behaviour which is initially characterized by a significantly hardening behaviour and successively by a rapidly softening behaviour;
- Brass on steel interface exhibited a quite low value of the friction coefficient and a stable behaviour characterized by a significant hardening;
- Material SA-21, which is a rubber based material developed for electrical machines, exhibited pinching behavior, low friction coefficient and a rapidly degrading behavior;

- Material STR-396, which is a hard rubber based material developed for applications where low wearing is necessary, developed a quite low value of the friction coefficient, but a very stable behavior and high energy dissipation capacity.

After the first phase devoted to the evaluation of the dissipative characteristics of the friction interfaces, an application of the same materials to beam-to-column joints equipped with such friction dampers has been proposed. In particular, the design process of the tested joints has been reported, showing the possibility of applying the component method as a design tool able to govern the failure mode and the energy dissipation supply of the proposed joint typology.

The experimental program dealing with double split friction tee stub joints has confirmed the possibility to obtain damage-free connections. The obtained results on the connections substantially confirm the results coming out from the tests on the friction dampers, pointing out the ability of the proposed joints to dissipate an high amount of energy without any damage to the structural parts. The results deriving from the experimental analysis have also been compared to that of a traditional DST joint tested in a past research program showing the effectiveness of the proposed joint when compared to traditional joint details. Even though the proposed technology still deserves further investigations, the results obtained appear very promising in order to apply free from damage connections in seismic design of steel moment resisting frames.

Regarding the cost of the proposed connection typology, even though this issue is outside the aim of the presented work, it is important to underline that it is expected that connections equipped with friction dampers are less expensive than traditional full-strength beam-to-column connections, because in this last case a significant overstrength with respect to the connected beam is needed, requiring the use of reinforcing ribs, cover plates, haunches or other elements to strengthen the connections. Notwithstanding this, if cost-benefit issues are considered, it is evident that the main advantage of the proposed connection typology is that it is a non-yielding connection which does not require any repair in the earthquake aftermath. However, as already pointed out, the attainment of the goal of non-yielding connections does not mean that buildings so designed are free from damage, because, on one hand, the connections proposed are not able to snap back to the original configuration, resulting in a permanent drift requiring a recentering in the aftermath of earthquake, and, on the other hand, large damage could potentially result to non-structural components, as result of transient drift, unless they are designed to accommodate such displacements.

## REFERENCES

- ANSI-AISC 341-10 (2010). *Seismic Provisions for Structural Steel Buildings*. American Institute of Steel Construction, Chicago, Illinois.
- Aribert, J., & Grecea, D. (2000). Numerical investigation of the q-factor for steel frames with semi-rigid and partial-strength joints. *Proceedings of the 3d International Conference STESSA 2000*. Montreal.
- Astaneh-Asl, A., & Nader, N. (1994). Proposed code provision for seismic design of steel semi-rigids and rigid frames. *Proceedings of the 5th U.S. National Conference of Earthquake Engineering (EERI)*. Chicago.
- Awkar, J., & Lui, E. (1999). Seismic Analysis and Response of Multistorey Seimirigid Frames. *Journal of Structural Engineering - ASCE*, 21, 1865-1872.
- Bernuzzi, C., Zandonini, R., & Zanon, P. (1996). Experimental analysis and modelling of semi-rigid steel joints under cyclic reversal loading. *Journal of Constructional Steel Research*, 2, 95-123.
- Carter, C., & Iwankiw, N. (1998). Improved ductility in seismic steel moment frames with dogbone connections. *Journal of Constructional Steel Research*, 46 (1-3), 253.
- Castro, J., Elghazouli, A., & Izzudin, B. (2005). Modelling of the panel zone in steel and composite moment frames. *Engineering Structures*, 27, 129-144.
- CEN. (2005a). *Eurocode 8: Design of structures for earthquake resistance - Part 1: General rules, seismic actions and rules for buildings*.
- CEN. (2005b). *Eurocode 3: Design of steel structures - Part 1-1: General rules and rules for buildings*.
- CEN. (2005c). *Eurocode 3: Design of steel structures - Part 1-8: Design of joints*.
- Chen, S. J., Yeh, C. H., and Chu, J. M. (1996). Ductile steel beam-to- column connections for seismic resistance. *Journal of Structural Engineering*, ASCE, Vol. 122, No. 11, pp. 1292-1299
- Chi, B. & Uang, C-H. (2002). Cyclic Response and Design Recommendations of Reduced Beam Section Moment Connections with Deep Columns. *Journal of Structural Engineering*, ASCE, Vol. 128, No. 4, pp. 464-473, April 1, 2002.
- Clemente, I., Noè, S., & Rassati, G. (2004). Experimental behavior of T-stub connection components for the mechanical modeling of Bare-Steel and composite partially restrained beam-to-column connections. *Proceedings of Connections in Steel Structures V*. Amsterdam.
- CNR-UNI 10011 (1997). *Costruzioni in acciaio: Istruzioni per il calcolo, l'esecuzione, il collaudo e la manutenzione*. Ente Nazionale Italiano di Unificazione, Milano.

- D'Aniello, M., Landolfo, R., Piluso, V., & Rizzano, G. (2012). Ultimate behavior of steel beams under non-uniform bending. *Journal of Constructional Steel Research*, 78, 144-158.
- Dubina, D., Muntean, N., Stratan, A., Grecea, D., & Zaharia, R. (2008). Testing program to evaluate behavior of dual steel connections under monotonic and cyclic loading. *Proceedings of the 5th European Conference on Steel and Composite Structures*. Graz, Austria.
- Engelhardt, M., Winneberger, T., Zekany, A., & Potyraj, T. (1997). Experimental investigation of dogbone moment connections. *Proceedings of National Steel Construction Conference*. Chicago: AISC.
- Ermopoulos, J., & Stamatopoulos, G. (1996). Analytical Modeling of Column Base Plates under Cyclic Loading. *Journal of Constructional Steel Research*, 40 (3), 225-238.
- Faella, C., Piluso, V., & Rizzano, G. (1998). Cyclic Behaviour of Bolted Joint Components. *Journal of Constructional Steel Research*, 46.
- Faella, C., Piluso, V., & Rizzano, G. (2000). *Structural Steel Semi-Rigid Connections*. Boca Raton: CRC Press.
- Fontana (2004): "Catalogo Tecnico – Prescrizioni Tecniche Bulloneria", Gruppo Fontana.
- Grecea, D., Dinu, F., & Dubina, D. (2004). Performance Criteria for MR Steel Frames in Seismic Zones. *Journal of Constructional Steel Research*, 60, 739-749.
- Heistermann, C. (2011). *Behaviour of Pretensioned Bolts in Friction Connections*. Lulea: Lulea University of Technology.
- Iannone, F., Latour, M., Piluso, V., & Rizzano, G. (2011). Experimental Analysis of Bolted Steel Beam-to-Column Connections: Component Identification. *Journal of Earthquake Engineering*, 15 (2), 214-244.
- Inoue, K., Suita, K., Takeuchi, I., Chusilp, P., Nakashima, M., Zhou, F. (2006). Seismic-Resistant Weld-Free Steel Frame Buildings with Mechanical Joints and Hysteretic Dampers. *Journal of Structural Engineering, ASCE*, Vol. 132, No. 6, pp. 864-872
- Jaspart, J. (1991). *Etude de la semi-rigidite des noeuds Poutre-Colonne et son influence sur la resistance et la stabilite des ossature en acier* (PhD Tesis ed.). Liege: University of Liege, Belgium.
- Kato, B. (1989). Rotation Capacity of H-section members as determined by local buckling. *Journal of Construction Steel Research*, 13, 95-109.
- Kim, K., & Engelhardt, M. (2002). Monotonic and cyclic loading models for panel zones in steel moment frames. *Journal of Constructional Steel Research*, 58, 605-635.

- Kim, Y., Ryu, H., & Kang, C. (2007). Hysteretic Behaviour of Moment Connections with Energy Absorption Elements at Beam Bottom Flanges. *ICAS 2007*. Oxford.
- Kishiki, S., Yamada, S., Suzuki, K., Saeki, E., Wada, A. (2006). New Ductile Moment-Resisting Connections Limiting Damage to Specific Elements at the Bottom Flange. Proceedings of the 8th National Conference on Earthquake Engineering, April 18-22, 2006, San Francisco, California, USA, paper No. 852.
- Koetaka, Y., Chusilp, P., Zhang, Z., Ando, M., Suita, K., Inoue, K., Uno, N. (2005). Mechanical Property of Beam-to-Column Moment Connection with Hysteretic Dampers for Column Weak Axis. *Engineering Structures*, Vol. 27 (2005), pp. 109-117.
- Latour, M., & Rizzano, G. (2013b). A Theoretical Model for Predicting the Rotational Capacity of Steel Base Joints. *Journal of Constructional Steel Research* , 91, 88-99.
- Latour, M., & Rizzano, G. (2012). Experimental Behavior and Mechanical Modeling of Dissipative T-Stub Connections. *Journal of Structural Engineering* , 138 (2), 170-182.
- Latour, M., & Rizzano, G. (2013a). Full Strength Design of Column Base Connections accounting for Random Material Variability. *Engineering Structures* , 48, 458-471.
- Latour, M., Piluso, V., & Rizzano , G. (2011). Cyclic Modeling of Bolted Beam-to-Column Connections: Component Approach. *Journal of Earthquake Engineering* , 15 (4), 537-563.
- Lignos, D. G., and Krawinkler, H. (2007). "A database in support of modeling of component deterioration for collapse prediction of steel frame structures." Proc., ASCE Structures Congress, ASCE, Reston, Va.
- Nogueiro, P., Simoes da Silva, L., Bento, R., & Simoes , R. (2009). Calibration of Model Parameters for the Cyclic Response of End-Plate Beam-to-Column Steel-Concrete Composite Joints. *Journal of Steel and Composites Structures* , 9 (1), 35-58.
- Oh, S.-H., Kim, Y.-J., Ryu, H.-S (2009). Seismic Performance of Steel Structures with slit dampers. *Engineering Structures*, Vol. 31 (2009), pp. 1997-2008.
- Piluso, V., & Rizzano, G. (2008). Experimental Analysis and modelling of bolted T-stubs under cyclic loads. *Journal of Constructional Steel Research* , 64, 655-669.
- Ramirez, C.M., Lignos, D.G., Miranda, E., Kolios, D. (2012). Fragility functions for pre-Northridge welded steel moment-resisting beam-to-column connections. *Engineering Structures*, Vol. 45 (2012) pp. 574-584.
- Ricles, J. M., Zhang, X., Lu, L. W., and Fisher, J. (2004). "Development of seismic guidelines for deep-column steel moment connections. Rep. No. 04-13, ATLSS Center, Lehigh Univ., Bethlehem, Pa.

- Schnorr. (2003). *Handbook for Disc Springs*. (E. F. Kleiner, Ed.) Heilbronn: Adolf Schnorr GmbH.
- Suita, K., Inoue, K., Takeuchi, I., Uno, N. (2004). Mechanical Joint with Hysteretic Dampers as Bolted Beam-to-Column Moment Connection. 13<sup>th</sup> World Conference on Earthquake Engineering. Vancouver, B.C. Canada, August 1-6, 2004, paper No. 225.
- Uang, C. M., and C. Bondad (1996). Static Cyclic Testing of Pre-Northridge and Haunch Repaired Steel Moment Connections. Report No. SSRP-96/02. San Diego, California: University of California, Division of Structural Engineering.
- Whittaker, A. S., A. Gilani and V. V. Bertero (1996). Seismic Testing of Full-Scale Beam-Column Assemblies. Part 1. SAC Report 96-01 (March). Sacramento, California: SAC Joint Venture Partnership.
- Yu, Q. S., Gilton, C., and Uang, C.-M. (2000). Cyclic response of RBS moment connections: Loading sequence and lateral bracing effects. Rep. No. SSRP-99/13, Dept. of Structural Engineering, Univ. of California, San Diego, California.